Ligand Field States and Vibrational Modes of Solid and Molten Elpasolite: $Cs_2NaHoCl_6$

Angelos G. Kalampounias and George N. Papatheodorou

Foundation for Research and Technology, Hellas-Institute of Chemical Engineering and High Temperature Chemical Processes, FORTH/ICE-HT, P.O. Box 1414, GR-26504, Patras, Greece and Department of Chemical Engineering, University of Patras, GR-26504, Patras, Greece

Reprint requests to Prof. G. N. P.; E-mail: gpap@iceht.forth.gr

Z. Naturforsch. **62a,** 169 – 175 (2007); received February 13, 2007

Presented at the EUCHEM Conference on Molten Salts and Ionic Liquids, Hammamet, Tunisia, September 16 – 22, 2006.

Electronic absorption and Raman spectra of solid and molten $Cs_2NaHoCl_6$ elpasolite have been measured in the temperature range 20 – 780 °C. The Raman spectra of the solid indicate that there is no phase transition above room temperature. It appears, that the internal vibrational modes of the solid are transferred into the melt, indicating that the $[HoCl_6]^{3-}$ "octahedra" are the predominant species. The $^5G_6 \leftarrow {}^5I_8$ and $^3H_6 \leftarrow {}^5I_8$ hypersensitive transitions of Ho(III) in elpasolite have been studied and analyzed in terms of the ligand field splittings of these states in the octahedral $[HoCl_6]^{3-}$ field. The temperature-induced changes in the spectra are attributed to the presence of "hot" bands arising from sets ("zones") of energy levels in the ground $^5I_8$ state. The continuous and smooth spectral changes observed upon melting indicate the presence of $[HoCl_6]^{3-}$ octahedra in both phases.

Key words: Molten Salts; Raman; Electronic Absorption; Ho(III); Hypersensitive Transition; Structure; Elpasolite.

1. Introduction

Over the past forty years a large number of compounds with the general formula M_2ALnX_6, where M and A are alkali metals with ionic radii $r_{M^+} > r_{A^+}$, Ln is a trivalent metal (rare-earth metal, actinide, Fe, Al), and X is a halide, have been synthesized and found to be isostructural. They bear the name elpasolites from the mineral K_2NaAlF_6. Early studies of the chloride elpasolites $Cs_2NaLnCl_6$ (Ln = Am [1], Bk [2], Fe [3], rare-earth metal [3]) have shown that these crystalline compounds are face-centered cubic with high space group symmetry $Fm\bar{3}m$ (O_h^5). The Ln(III) cations are located at octahedral sites in six-fold coordination with Cl^- anions. The Cs^+ cations form a simple cubic lattice while the Na^+ cations are also at an octahedral site. There is practically no Ln–Ln interaction since these cations are fourth-nearest neighbours, thus "independent" $[LnCl_6]^{3-}$ octahedra which are surrounded by the highly symmetric field of the A and M cations have an "ideal" O_h symmetry.

Based on this high symmetry around the Ln(III), elpasolite crystals have been used extensively to study the spectra and energy levels of the lanthanides in octahedral coordination, especially at cryogenic temperatures. A comprehensive review on this subject has recently been published [4].

The rather simple vibrational modes of these high symmetry crystals [5] permit by IR and Raman measurements the determination of the vibrational frequencies of many $[LnX_6]^{3-}$ octahedra [6]. Furthermore, systematic studies of the vibrational-Raman spectra of many chloride, bromide and fluoride elpasolites as solids at different temperatures and as melts have contributed to the understanding of the structure of a large number of molten rare-earth halides (LnX_3) and their mixtures with alkali halides (AX) of the type LnX_3-ACl [7] with X = F [8], Cl [5, 9, 10] and I [11].

More recently, the structural properties of the $LnCl_3$-ACl melt mixtures have been investigated by electronic absorption spectroscopy using the f ← f transitions of Ho(III) dissolved in the mixture as probe cation. The spectra of dilute solutions of Ho(III) in molten $GdCl_3$-KCl [12] and $LaCl_3$-KCl [13] mixtures were measured at different compositions and temperatures. It appeared that the Ho(III) coordination in these

melts is six-fold, and that the energies and relative intensities of the ligand field components involved in the $^5G_6 \leftarrow {}^5I_8$ hypersensitive transition depend on the degree of octahedral distortion of the $[HoCl_6]^{3-}$ species. However, it was not possible to establish with certainty the high temperature absorption spectra of the well-defined $[HoCl_6]^{3-}$ octahedra.

The present work deals with the f ← f electronic absorption spectra of Ho(III) in solid and molten elpasolite $Cs_2NaHoCl_6$. Emphasis is given to the $^5G_6 \leftarrow {}^5I_8$ and $^3H_6 \leftarrow {}^5I_8$ hypersensitive transitions and the temperature dependence of the ligand field bands arising from f electron splitting in the octahedral field. Raman spectroscopic measurements establish the presence of $[HoCl_6]^{3-}$ "octahedra" as the predominant species in molten elpasolite and thus the electronic absorption spectra obtained from this melt can be used as a "finger print" in characterizing the spectral behaviour of Ho(III) in the above-mentioned molten salt mixtures $GdCl_3$-KCl [12] and $LaCl_3$-KCl [13] as well as other melts.

2. Experimental

High purity anhydrous $HoCl_3$, NaCl and CsCl were purchased from Alfa and were further purified as before [9]. All anhydrous materials were handled in a nitrogen atmosphere glove box and/or in sealed fused silica tubes. The elpasolite $Cs_2NaHoCl_6$ was prepared by transferring appropriate amounts of the component salts into a fused silica tube (∼ 10 cm long, ∼ 8 mm OD) sealed at one end. The tube was then evacuated, torch-sealed at the other end and placed in a furnace at ∼ 900 °C, where a uniform and clear melt was obtained. Cooling of the melt gave the elpasolite in polycrystalline form. About 200 mg of the compound were placed and sealed in a Raman cell made from a ∼ 3 mm ID, 5 mm OD silica tube. A modified Jobin-Yvon (model T-6400) Raman system, equipped with a high temperature furnace, was used for measuring the spectra of the polycrystalline solid and the melt as before [7].

The electronic absorption spectra were measured with a Perkin Elmer (model Lambda 900) spectrophotometer equipped with a home-made optical furnace [12, 13]. The spectrophotometer operated with reverse optics having the configuration: light source → sample → monochromator → detector. This configuration eliminates from the spectra the background arising from the black body radiation emitted from the furnace at high temperatures. The procedures for measuring the absorption spectra were the following: Fused silica optical cells (Ultrasil, Starna, UK) with path lengths of 0.05 cm and a cylindrical tube (∼ 8 mm OD), sealed on the top, were used. Solid elpasolite was introduced and the cell was evacuated and torch-sealed on the top of the tube. Then, the solid was melted in a furnace and the liquid was forced by shaking the cell to fill uniformly the lower part of the cell (0.05 cm path length, ∼ 4 cm height and ∼ 1 cm width). Then, while hot at ∼ 850 °C, the cell was introduced into the spectrophotomer furnace, whose temperature was ∼ 10 °C above melting. After equilibrating at this temperature, the melt spectra were measured at ∼ 780 °C, and then the temperature was slowly reduced by ∼ 5 degrees, where the melt was solidified as a transparent clear *plate* (0.05 cm thick) within the optical cell. Further, slow and gradual lowering of the temperature permitted spectral measurements of the solid at different temperatures down to the ambient temperature. Partial cracking of the clear solid plate occurred below ∼ 400 °C, resulting in an increasing background which could be subtracted, and thus the absorbance of the Ho(III) transitions could still be measured.

The calculation of molar absorptivity requires knowledge of the density (molar volume) of both molten and solid $Cs_2NaHoCl_6$. To our knowledge such data are not available; thus we have estimated the densities of the two phases as follows: From the lattice parameter of the elpasolite $a \approx 10.725$ Å [3] the density of the solid was found as $d_{\text{solid}} \approx 3.67$ g/cm^3. Assuming that the molar volume of the melt is a superposition of the molar volumes of the component salts, the melt density is $d_{\text{melt}} \approx 2.5$ g/cm^3. To verify this value we have also estimated experimentally the molar volume of molten elpasolite by melting known amounts of the salt in small fused silica tubes (3 mm ID) and measuring the height of the melt in the tube. A value of ∼ 2.4 g/cm^3 was found, which is close to the above calculated value.

3. Results and Discussion

3.1. Vibrational Modes

An analysis of the distribution of normal modes for the elpasolite structure ($Fm\bar{3}m - O_h^5$) gives [5]:

$$\Gamma_{3N} = \Gamma_{\text{acoustic}} + \Gamma_{\text{translatory}} + \Gamma_{\text{libration}} + \Gamma_{\text{internal}},$$

$$\Gamma_{\text{acoustic}} = T_{1g}(\text{IR}),$$

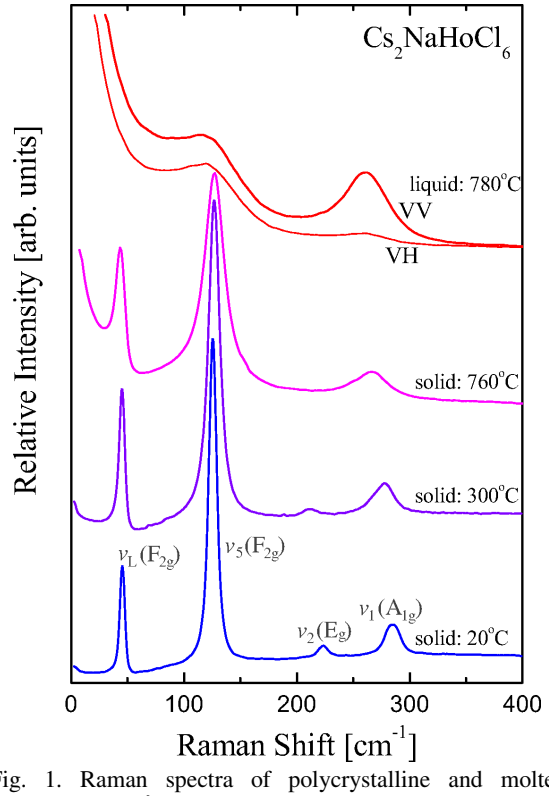

Fig. 1. Raman spectra of polycrystalline and molten $Cs_2NaHoCl_6$. $\lambda_o = 514.5$ nm; spectral resolution = 1.5 cm^{-1}; laser power = 300 mW; CCD detector.

$$\Gamma_{\text{translatory}} = T_{2g}(\text{R}) + 2T_{1u}(\text{IR}),$$
$$\Gamma_{\text{libration}} = T_{1g}(\text{IA}),$$
$$\Gamma_{\text{internal}} = A_{1g}(\text{R}) + E_g(\text{R}) + T_{2g}(\text{R}) + 2T_{1u}(\text{IR}) + T_{2u}(\text{IA}).$$

The internal modes correspond to the $[HoCl_6]^{3-}$ octahedral vibrational modes from which three are Raman-active. Thus, with the additional acoustic mode a total of four Raman-active modes are expected and are clearly seen in the room temperature spectra (Fig. 1). The frequencies of the peaks observed in the Raman spectra at different temperatures and their assignments are given in Table 1. The assignement of the internal modes is unique since the frequencies extrapolated to ~ 0 K satisfy the relation [14] $\nu_1^2 \approx \nu_2^2 + \frac{3}{2}\nu_5^2$.

With increasing temperature all the bands seen in the solid at 20 °C become broader, the stretching modes ν_1 and ν_2 are shifted to lower energies while the pure bending mode [6] and the lattice mode are practically insensitive to the temperature (Fig. 1, Table 1). At high temperatures, the low intensity ν_2 band is overcome by the neighbouring bands due to broadening. The observed bands at different temperatures and the minor frequency shifts observed indicate that the elpasolite structure remains cubic at all temperatures above room temperature.

Table 1. Raman frequencies (cm^{-1}) and assignments of solid and liquid $Cs_2NaHoCl_6$.

Temperature [°C]	$\nu_1(A_{1g})$	$\nu_2(E_g)$	$\nu_5(T_{2g})$	$\nu_L(T_{2g})$
20	285	224	126	45
300	278	212	126	45
760	267	–	125	43
780 (melt)	(264)[a]	–	(134)[a]	–

[a] Measured from reduced Raman spectra [7].

The overall effect regarding the "red" shift of the $\nu_1(A_{1g})$ band, which occurs by raising the solid temperature is attributed as before [7] to the weakening of the Ho-Cl bonding. Furthermore, the fact that the frequency of the pure bending mode $\nu_5(T_{2g})$ is not affected by the temperature indicates that the octahedral 90° angles do not change, or in other words that the "ideal" $[HoCl_6]^{3-}$ octahedral units are preserved at high temperatures.

Upon melting there is a further frequency "red" shift of the $\nu_1(A_{1g})$ band, which is polarized, while the lattice mode is replaced by the depolarized liquid wing [7] on the tale of which the depolarized $\nu_5(T_{2g})$ mode is superimposed. The observed bands in the melt, their polarization characteristics and their systematics in relation to the bands seen in the solid at high temperature are considered to indicate that the $[HoCl_6]^{3-}$ internal modes of the solid are preserved in the melt. Furthermore, all the $LnCl_3$-ACl melt mixtures studied so far by thermodynamic [15 – 17], Raman spectroscopic [7, 10], and computer simulation [18, 19] methods show that in melts rich in ACl (as in the case of molten elpasolites) the *predominant* species present are the $[LnCl_6]^{3-}$ "octahedra". It is noteworthy that the ionic radius of Ho(III) is almost identical with that of Y(III), and that YCl_3 and $HoCl_3$ are isomorphous solids. The YCl_3-ACl melt systems were well studied [5, 16, 19] and confirm the presence of $[YCl_6]^{3-}$ octahedra in the ACl-rich melts. In other words, we can conclude with certainty that $[HoCl_6]^{3-}$ is the predominant species formed in molten elpasolite processing the octahedral "internal" modes of vibration which are seen in the Raman spectra.

3.2. f-Electron Ligand Field States

Typical absorption spectra of Ho(III) in solid and molten elpasolite are shown in Figure 2. The assign-

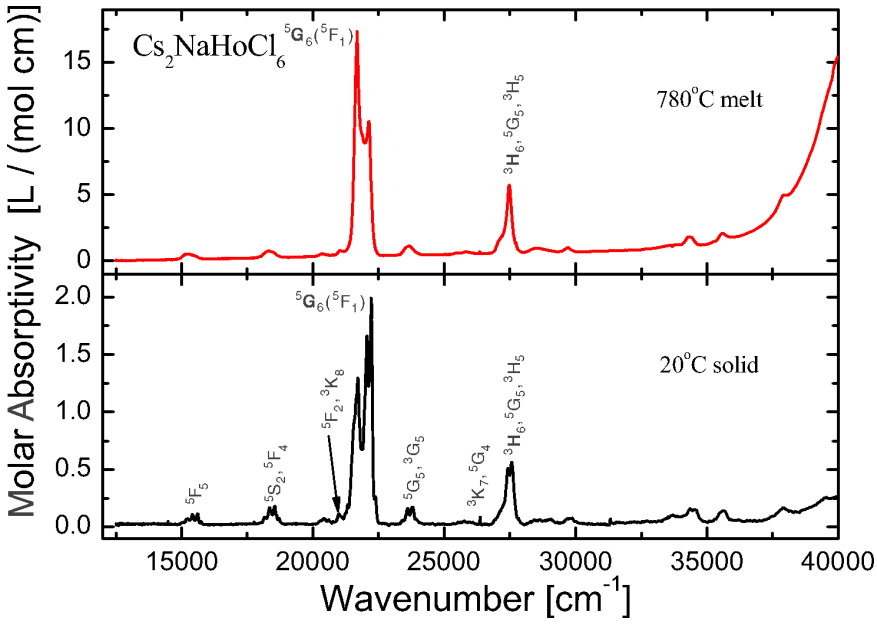

Fig. 2. Molar absorptivity spectra of Ho(III) in solid (20 °C) and molten (780 °C) $Cs_2NaHoCl_6$. The assignments of certain Ho(III) free ion states marked on the spectra are from [20].

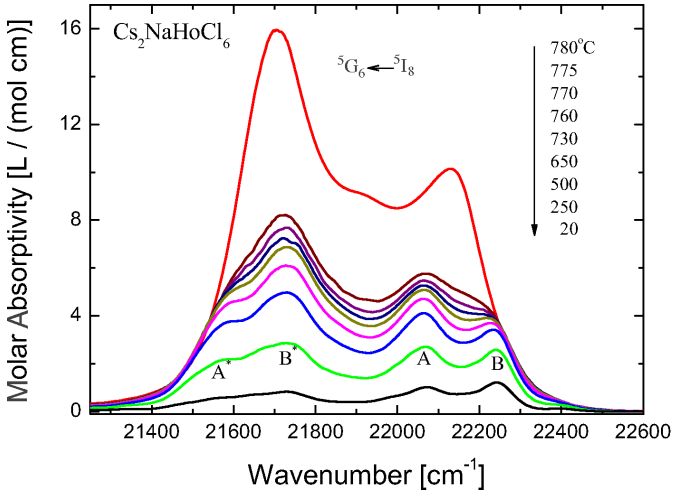

Fig. 3. Expanded spectra of the ligand field transitions associated with the $^5G_6 \leftarrow {}^5I_8$ hypersensitive transition of Ho(III) in solid and molten $Cs_2NaHoCl_6$.

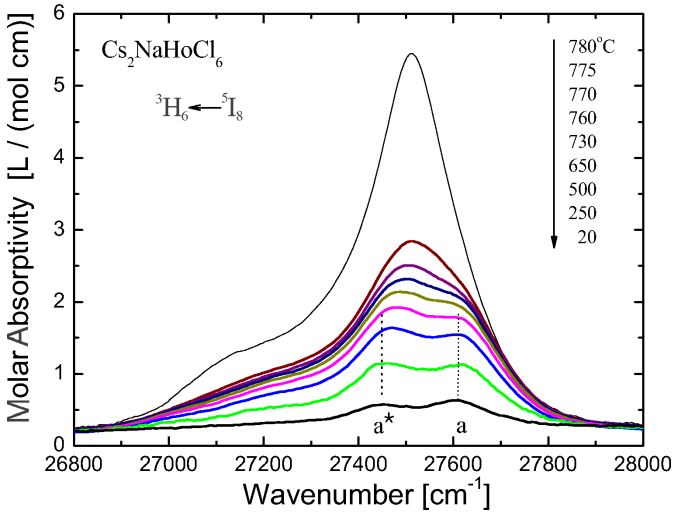

Fig. 4. Expanded spectra of the ligand field transitions associated with the $^3H_6 \leftarrow {}^5I_8$ hypersensitive transition of Ho(III) in solid and molten $Cs_2NaHoCl_6$.

ments given on the top of the spectra are for the free ion states and are based on [20]. The two more intense bands seen in the spectra are the hypersensitive transitions $^5G_6 \leftarrow {}^5I_8$ and $^3H_6 \leftarrow {}^5I_8$ [21]. In the octahedral field of the chloride ions the free ion Ho(III) f states split into components which can be better identified in expanded spectra.

These ligand field components are easily recognized for the two hypersensitive transitions as shown in Figs. 3 and 4 from room temperature up to above melting. It has been argued [20, 21] that the main factors affecting the hypersensitive transition intensities (i. e. oscillator strength / molar absorptivity) in an octahedral $[LnX_6]^{3-}$ species are the degree of distortions from ideal O_h symmetry in conjunction with the overall change asymmetry and polarizability around the lanthanide metal. The Boltzman thermal population effect on the ground state levels alters the intensities in certain cases; thus Ho(III) is also responsible for the appearance of intense "hot" bands in the spectra. Furthermore, for an octahedral species possessing a centre of symmetry, the forced electric dipole transitions are expected to show vanishing intensities [22]. This indeed often occurs at cryogenic temperatures, where the elpasolites have the $[LnX_6]^{3-}$ octahedra in an "ideal" coordination. The room temperature spectra also show (Figs. 3, 4) rather small molar absorptivities.

On the other hand, vibronic coupling with mainly the odd $\nu_3(T_{1u})$, $\nu_4(T_{1u})$ and $\nu_6(T_{2u})$ vibrational modes of the octahedral (see previous subsection) as well as static thermal distortions break the inversion symmetry and enhance the f $\leftarrow$ f transition intensities especially at elevated temperatures. Thus, the overall intensity of the solid is expected to increase with temperature and this accounts for the spectral changes seen in Figs. 3 and 4.

The energy of the ligand field states of Ho(III) in solid elpasolite has been established through electronic absorption and emission spectroscopic measurements mainly at cryogenic temperatures and up to room temperature, as well as with theoretical calculations [23, 24]. For the states involved in the hypersensitive transition $^5G_6 \leftarrow {}^5I_8$ the octahedral ligand field energies are shown schematically in Figure 5. The magnitude of the ground state ($^5I_8$) splitting is lower than the kT value corresponding to 600 K (~ 420 cm^{-1}), which implies that in the temperature range of our experiments (~ 600 to 1000 K) all the splitting components of the ground state would be accessible by the Boltzmann thermal distribution of the states and would contribute as broad energy states to the hypersensitive transitions. Certain states in Fig. 5 with small energy differences have been grouped to four "zones" marked as ε_0, ε_0^*, ε_1 and ε_1^*. Thus, combination of four electronic transitions from the two "zones" in the ground state to the two "zones" in the excited state are expected to give rise to the spectra in Figure 3. However, due to the vibronic character of the f $\leftarrow$ f transitions, the excited state ("zone") should involve the odd vibrational frequencies of $[HoCl_6]^{3-}$ which are experimentally known [23, 25]:

$$\nu_3(T_{1u}) \approx 255 \text{ cm}^{-1}; \quad \nu_6(T_{2u}) \approx 108 \text{ cm}^{-1};$$
$$\nu_4(T_{1u}) \approx 86 \text{ cm}^{-1}.$$

Thus, the overall energy of the excited state "zones" should be raised by $\sim \nu_4$ (86 cm^{-1}) and their width raised by $(\nu_3 - \nu_4) \approx 170$ cm^{-1}, as approximately shown in Figure 5. It is thus more likely that in the high temperature Ho(III) elpasolite spectra four bands should appear with strongly overlapping tails due to the energy width of the "zones" involved. These transitions are marked in Fig. 5 as A, A*, B, B*, and their relative average energies estimated from [23] were found to increase in the order A* < B* < A < B. We *tentatively* assign these bands to the four main bands measured for the $Cs_2NaHoCl_6$ as seen in Figure 3. As expected from the Boltzmann distribution in the spectra region of the "hot" bands A*, B*, the intensity (molar absorptivity) increases with temperature relative to the intensity of the A, B bands. On the other hand, the relative intensity changes with temperature of the A and B bands are puzzling. Furthermore, calculations of the dipole strength [23] for the transitions involving the three ligand field states (^aE_g, $^aT_{1g}$, A_{1g}) of the ε_0 "zone" and the states of the ε_1 and ε_1^* "zones", as well as band intensity calculations [23] for the same transitions indicate that (at ~ 10 K) the intensity of the B band should be much lower than that of the A band. In contrast, at room temperature these bands have comparable molar absorptivities (Fig. 3), and at higher temperature the A band dominates this region of the spectra.

The ligand field states of $^3H_6$ state involved in the second hypersensitive transition of $Cs_2NaHoCl_6$ (Fig. 4) have been recently calculated [26]. Six Stark components spread between ~ 27950 and 27600 cm^{-1} have been found which cannot be grouped into smaller "zones" as before. Thus, taking into account the further spread of these states due to the odd vibrations, we would expect that at high temperatures a broad ex-

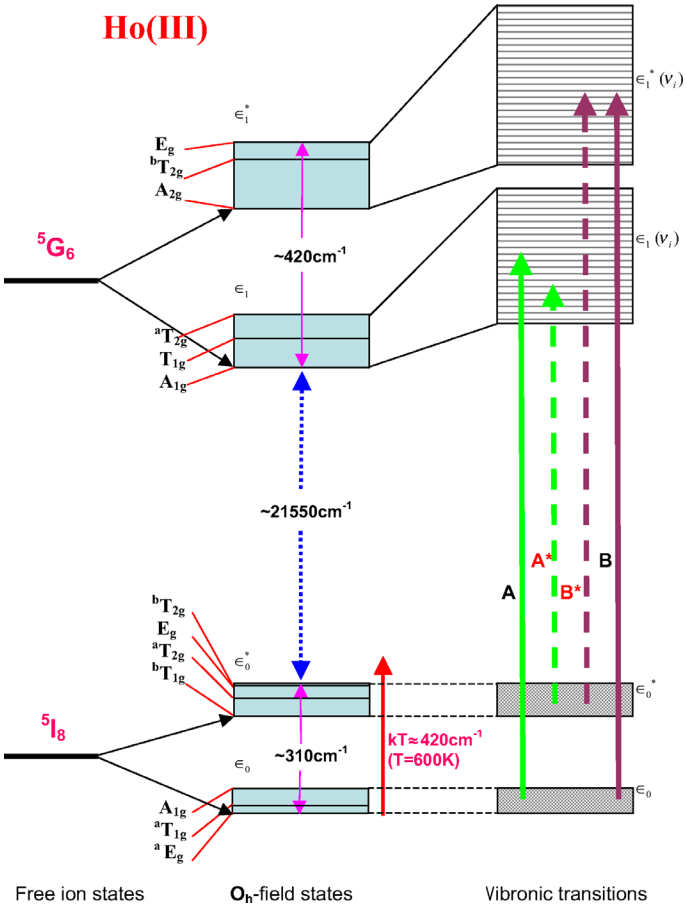

Fig. 5. Schematic diagram of the ligand field states arising from the ground and excited states involved in the $^5G_6 \leftarrow {}^5I_8$ hypersensitive transition of Ho(III) in elpasolite. The energy differences between the "free" ion states are not on scale, but within each state the "zone" widths and separations are comparable to each other and to the kT value shown as a vertical arrow. For other details see text.

cited state covers all these states and thus, two main transitions are possible:

Band a : $^3H_6$ [all states] $\leftarrow {}^6I_8$ ["zone" ε_0],
Band a* : $^3H_6$ [all states] $\leftarrow {}^6I_8$ ["zone" ε_0^*].

Again, with increasing temperature the "hot" band a* gains intensity (Fig. 4), and this supports the above assignment. The appearance at high temperature in the solid (and melt) spectra of a third lower energy band ($\sim 27100\,\mathrm{cm}^{-1}$) is more likely to involve transitions to the ligand field states of the neighbouring $^5G'_5$ state [26].

As established by the Raman spectra, there are no phase transitions of the solid $Cs_2NaHoCl_6$ above room temperature and temperature-induced changes on the absorption spectra are rather smooth, as seen in Figs. 3 and 4. These rather continuous spectral changes observed in the solid appear to be passed into the melt. The band positions and relative intensity changes are also smoothly transferred into the melt, while the molar absorptivity is almost doubled upon melting (Figs. 3 and 4). A new weak band appears at $\sim 21900\ \mathrm{cm}^{-1}$, and the overall spectra (intensities and band positions) are close to those measured in molten alkali chlorides [12, 13]. As shown in the previous section, the Raman spectra and other physicochemical methods suggest that the $[HoCl_6]^{3-}$ "octahedra" are preserved upon melting the elpasolite and are the predominant complex ionic species formed in dilute solutions of Ho^{3+} in molten alkali chlorides. In other words, it appears that the $^5G_6 \leftarrow {}^5I_8$ and $^3H_6 \leftarrow {}^5I_8$ spectra of Ho(III) in molten elpasolite (as well as in molten alkali chlorides) are associated with transitions arising from the ligand field components of Ho(III) in an "octahedral" coordination. The rather abrupt increase of the molar absorptivity as we go from the solid to the melt is attributed to octahedral distortions which deviate the $[HoCl_6]^{3-}$ from centro-symmetry, and thus the dipole-induced transitions are partially allowed. Increasing the melt temperature enhances the octahedral distor-

tions, and this is reflected on the spectra by smooth band shifts and increasing band intensities, as it has been seen and discussed in the Ho(III) spectra in alkali chlorides [12, 13].

Finally, it should be pointed out that the ligand field spectra of Ho(III) coordinated with halide ligands change drastically from "trigonal" (HoX_3) to "tetrahedral" ($[HoX_4]^-$) to "octahedral" ($[HoX_6]^{3-}$, X = I [27], Cl [28]). For the $^5G_6 \leftarrow {}^5I_8$ transition the band positions, the relative intensities and the overall oscillator strengths depend strongly on the coordination geometry. This further supports the view that the solid and melt spectra seen in Fig. 4 are correlated and that both correspond to octahedral $[HoCl_6]^{3-}$ species.

4. Conclusions

Continuous temperature-induced changes have been observed in the electronic absorption and Raman spectra measured on solid and molten $CsNaHoCl_6$ elpasolite. The data indicate that the well-defined octahedral species in solid $[HoCl_6]^{3-}$ are also the predominant species in the melt.

Detailed examination of the electronic absorption spectra in the region of the $^5G_6 \leftarrow {}^5I_8$ and $^3H_6 \leftarrow {}^5I_8$ hypersensitive transition of Ho(III) show a number of broad and overlapping bands which are due to the ligand field splitting of the ground and excited states of these transitions. For each transition the relative intensity changes induced by the temperature are attributed to "hot" bands arising from sets ("zones") of energy levels in the ground state.

This work establishes the f ← f electronic absorption spectra of $[HoCl_6]^{3-}$ in the molten state and permits the use of Ho(III) as a probe ion for structural studies of melts and melt mixtures involving rare-earth halides.

[1] K. W. Bagnall, J. B. Laldler, and M. A. A. Stewart, J. Chem. Soc. A **133**, (1968).
[2] L. R. Morss and J. Fuger, Inorg. Chem. **8**, 1433 (1969).
[3] L. R. Morss, M. Siegal, L. Stenger, and N. Edelstein, Inorg. Chem. **9**, 1771 (1970).
[4] P. A. Tanner, Top. Curr. Chem. **241**, 167 (2004).
[5] G. N. Papatheodorou, J. Chem. Phys. **66**, 2893 (1977).
[6] K. Nakamoto, Infrared and Raman Spectra of Inorganic and Coordination Compounds, Parts I and II, Wiley, New York 1997.
[7] G. N. Papatheodorou and S. N. Yannopoulos, in: Molten Salts: from Fundamentals to Applications (Ed. M. Gaune-Escard), NATO ASI Symposium Series 2, Vol. 52, Kluwer, Boston 2002, p. 47 and references therein.
[8] V. Dracopoulos, B. Gilbert, and G. N. Papatheodorou, J. Chem. Soc. Faraday Trans. **94**, 2601 (1998) and references therein.
[9] G. M. Photiadis, B. Borresen, and G. N. Papatheodorou, J. Chem. Soc. Faraday Trans. **94**, 2605 (1998).
[10] G. Zissi and G. N. Papatheodorou, Phys. Chem. Chem. Phys. **6**, 4480 (2004).
[11] A. Chrissanthopoulos, G. D. Zissi, and G. N. Papatheodorou, Z. Naturforsch. **60a**, 739 (2005).
[12] A. Chrissanthopoulos and G. N. Papatheodorou, Phys. Chem. Chem. Phys. **2**, 7309 (2000).
[13] A. Chrissanthopoulos and G. N. Papatheodorou, J. Mol. Struct. **782**, 130 (2006).
[14] D. M. Yost, C. C. Steffins, and S. T. Cross, J. Chem. Phys. **2**, 311 (1933).
[15] G. N. Papatheodorou and T. Østvold, J. Phys. Chem. **78**, 181 (1974).
[16] G. N. Papatheodorou, O. Waernes, and T. Østvold, Acta Chem. Scand. A **33**, 173 (1979).
[17] M. Gaune-Escard, in: Molten Salts: from Fundamentals to Application (Ed. M. Gaune-Escard), NATO ASI Symposium Series 2, Vol. 25, Kluwer, Boston 2002, p. 375 and references therein.
[18] W. J. Glover and P. A. Madden, J. Chem. Phys. **121**, 7293 (2004) and references therein.
[19] F. Hutchinson, M. Wilson, and P. A. Madden, J. Phys.: Condens. Matter **12**, 10389 (2000).
[20] W. T. Carnall, P. R. Fields, and K. Rajnak, J. Chem. Phys. **49**, 4424 (1968) and references therein.
[21] C. Görllez-Walrand and K. Binnemans, in: Handbook of the Physics and Chemistry of Rare-Earths (Ed. K. A. Gschneidner Jr. and L. Eyring), Elsevier Science, Amsterdam 1998, Vol. 25, chapter 169, p. 101 and references therein.
[22] B. R. Judd, Phys. Rev. **127**, 750 (1962); G. S. Ofelt, J. Chem. Phys. **37**, 511 (1962).
[23] J. P. Morley, T. R. Faulkner, F. S. Richardson, and R. W. Schwarztz, J. Chem. Phys. **75**, 539 (1981).
[24] P. A. Tunner, V. V. Ravi Kanth Kumar, C. K. Jayasankar, and M. F. Reid, J. Alloys Comp. **215**, 349 (1994).
[25] X. Zhou and P. A. Tanner, Chem. Phys. Lett. **413**, 284 (2005).
[26] D. Wang, Y. Min, W. Zhang, D. Ning, Y. Zhang, and S. Xia, J. Alloys Comp. **361**, 1 (2003).
[27] G. N. Papatheodorou and A. Chrissanthopoulos, J. Mol. Struct. **832**, 38 (2007).
[28] A. G. Kalampounias and G. N. Papatheodorou, to be submitted.